Available online at www.sciencedirect.com
SCIENCE DIRECT®
International Journal of Heat and Mass Transfer 49 (2006) 671–681
International Journal of HEAT and MASS TRANSFER
www.elsevier.com/locate/ijhmt

Effect of oscillatory frequency on heat transfer in metal foam heat sinks of various pore densities

K.C. Leong *, L.W. Jin

School of Mechanical and Aerospace Engineering, Nanyang Technological University, 50 Nanyang Avenue, Singapore 639798, Republic of Singapore

Received 24 May 2005; received in revised form 17 August 2005
Available online 13 October 2005

Abstract

In this paper, an experimental investigation was performed to study the heat transfer performance of metal foam heat sinks of different pore densities subjected to oscillating flow under various oscillatory frequencies. The variations of pressure drop and flow velocity along the kinetic Reynolds number of oscillating flow through aluminum foams were compared. The measured pressure drops, velocities and surface temperatures of oscillating flow through aluminum 10, 20 and 40 PPI foams were presented in detail. The calculated cycle-averaged local temperature and Nusselt number for different kinetic Reynolds numbers were analyzed and compared with finned heat sinks. The results of length-averaged Nusselt number for both oscillating and steady flows indicate that higher heat transfer rates can be obtained in metal foams subjected to oscillating flow. For the purpose of designing a novel heat sink using metal foam, the characteristics of the pumping power of the cooling system for aluminum foam with different pore densities were also analyzed.

Keywords: Kinetic Reynolds number; Aluminum foam; Oscillating flow; Pressure drop; Pumping power

1. Introduction

Current integrated circuit and photonic technologies as well as the ubiquity of electronic system applications are providing a serious challenge to heat transfer science. Driven by the increase in spatial density of microelectronic devices, chip powers are increasing rapidly with resulting increase in the heat flux. The traditional approaches using plate-finned heat sink are becoming less viable as power levels increase. An innovative cooling method is needed to remove significant amounts of heat at high fluxes with compact and highly reliable devices. The porous medium with a large solid–fluid contact surface area and high thermal conductivity has emerged as an effective cooling method. To solve the issue of the thermal management in electronic components effectively, heat transfer characteristics in porous media have been investigated extensively in the past two decades [1–5].

As compared to the porous channel packed with metal particles, spheres or woven-screens, the open-cell metal foam fabricated by infiltration casting technique is a novel porous medium with a metal skeletal structure as shown in Fig. 1(a). Typically, it is manufactured by solidification of metal from a super-heated liquidus state in an environment of high pressure and high vacuum. A close-up view of the inside structure in Fig. 1(b) shows that the open-cell metal foam has a reticulated structure of open, shaped cells connected by continuous solid metal ligaments. The cell has the approximate shape of a tetrakaidecahedron, whose pentagonal or hexagonal faces are open to one another. The fully inter-connected pore and ligament structures provide the extreme large fluid-to-solid contact surface area, and tortuous coolant flow path inside the metal foam, which could increase dramatically the overall heat transfer rate. Lu et al. [6] and Bhattacharya and Mahajan [7] performed analytical and experimental studies, respectively

* Corresponding author. Tel.: +65 6790 5596; fax: +65 6792 2619.
E-mail address: mkcleong@ntu.edu.sg (K.C. Leong).

0017-9310/$ - see front matter © 2005 Elsevier Ltd. All rights reserved.
doi:10.1016/j.ijheatmasstransfer.2005.08.015

Nomenclature

A_{heated}	heated area (m^2)
C	constant
c_{pf}	specific heat of fluid ($J\,kg^{-1}\,K^{-1}$)
D_e	hydraulic diameter of the channel, $5H/3$
D_h	hydraulic diameter of the fin based on fin height
d_l	ligament diameter of porous media (μm)
f	oscillatory frequency (Hz)
H	height of the channel (m)
H_f	height of fin (m)
h_x	local heat transfer coefficient defined in Eq. (7)
K	permeability of the porous medium (m^2)
k_d	thermal dispersion conductivity defined in Eq. (9)
k_e	effective thermal conductivity of porous media ($W\,m^{-1}\,K^{-1}$)
k_f	thermal conductivity of fluid ($W\,m^{-1}\,K^{-1}$)
L	length of the test section (m)
Nu_x	cycle-averaged local Nusselt number defined in Eq. (6)
Nu_{avg}	length-averaged Nusselt number
Pe_e	effective local Peclet number defined in Eq. (10)
Pr	Prandtl number
ΔP	pressure drop across the test section (Pa)
ΔP_{max}	maximum pressure drop across the test section (Pa)
Q	power input (W)
Re	Reynolds number based on the hydraulic diameter of fin height
Re_ω	kinetic Reynolds number defined in Eq. (5)
S	fin spacing of heat sink (m)
t	time of oscillatory cycle (s)
T_{avg}	length-averaged surface temperature (°C)
T_w	cycle-averaged local surface temperature (°C)
T_i	cycle-averaged temperature at the inlet of test section (°C)
U	average flow velocity in porous media ($m\,s^{-1}$)
U_{max}	maximum flow velocity in porous media ($m\,s^{-1}$)
v_s	volume of solid fraction of the tested metal foam (m^3)
v_t	total volume of the tested metal foam (m^3)
$\dot{V}$	average maximum volumetric flow rate ($m^3\,s^{-1}$)
w	channel width (m)
W_p	maximum pumping power defined in Eq. (12)
X	location of thermocouples in the test section

Greek symbols

α	specific surface area of aluminum foam ($m^2\,m^{-3}$)
α^*	effective thermal diffusivity ($m^2\,s^{-1}$)
ω	angular frequency
ν_f	kinematic viscosity of fluid ($kg\,m^{-1}\,s^{-1}$)
ρ_f	density of fluid ($kg\,m^{-3}$)
δ	uncertainty
γ	thermal dispersion coefficient
ε	porosity of the metal medium
μ_f	dynamic viscosity of fluid ($m^{-2}\,s^{-1}$)

on forced convection in aluminum foam used as a heat sink. Their results showed that high heat transfer coefficients can be achieved by using a metal foam heat sink with relatively small pressure drop as compared to commercially available fin heat sink. Kim et al. [8] and Ko and Anand [9] investigated forced convection in a channel fully and partially inserted with various metal foams and reported high heat transfer performance. Boomsma et al. [10] experimentally studied the metal foam as a compact heat exchanger and pointed out that the open-cell aluminum foam generated thermal resistances that were two to three times lower than the best commercially available heat exchanger tested, while requiring the same pumping power.

However, uni-directional flow through the porous channel yields a relatively high temperature difference along the flow direction on the substrate surface [11,12]. For modern high-speed microprocessors, the reliability of transistors and operating speed are not only influenced by the average temperature but also by temperature uniformity on the substrate surface. Therefore, maintaining the uniformity of on-die temperature distribution below certain limits is imperative in thermal design. It is conceivable that oscillating flow through a porous channel will produce a more uniform temperature distribution due to the presence of two thermal entrance regions for oscillating flow. Sozen and Vafai [13] numerically analyzed the forced convection flow through a packed bed under oscillating compressible flow. The effect of oscillating boundary conditions on the transport phenomena in the packed bed was investigated and comparisons were made with the case of constant-temperature and constant-pressure boundary conditions. Guo et al. [14] investigated oscillating flow and heat transfer characteristics in a circular pipe partially filled with porous media. The enhanced longitudinal heat conduction due to oscillating flow and enhanced convective heat transfer from high conducting porous material were examined. Leong and Jin [15] studied the heat transfer of a channel filled with a metal foam subjected to oscillating flow. Their results showed that heat transfer performance in a channel can be enhanced substantially and that a more uniform temperature distribution can be obtained by inserting porous media subjected to oscillating flow. Leong and Jin [16] also analyzed the transient velocity and pressure drop profiles of oscillating flow through metal foam channel. They found that the phase difference between velocity and pressure drop is small for open-cell aluminum foams of high porosity.

The above review shows that research on metal foams as heat sinks were conducted mainly for the uni-directional

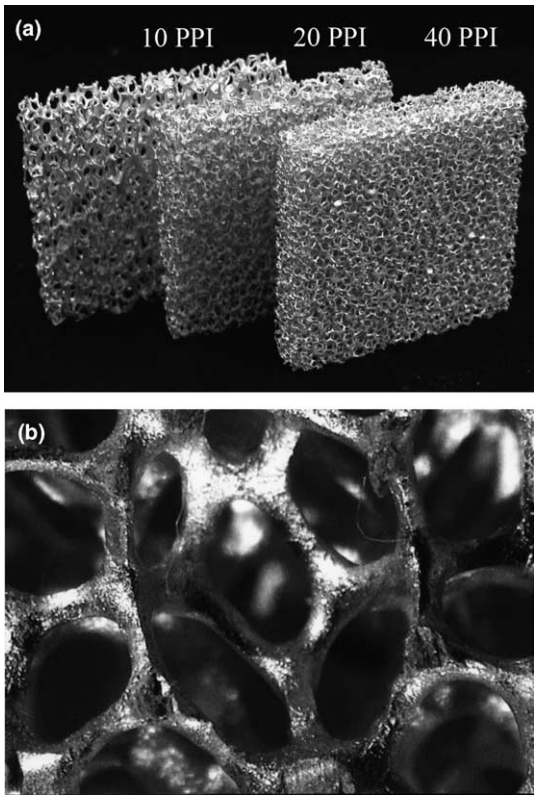

Fig. 1. (a) Aluminum open-cell foams and (b) typical pore structure of open-cell metal foam.

flow condition whilst published literature on metal foams as heat sinks subjected to oscillating flow is rather scarce. As a follow up on the authors' previous works [15,16] which showed that heat transfer characteristics of oscillating flow in metal foam are governed by the dimensionless flow amplitude and kinetic Reynolds number, further experimental investigations were performed on aluminum foams as heat sinks with different pore densities subjected to oscillating flow under various oscillatory frequencies. The cycle-averaged local temperature and Nusselt number with different kinetic Reynolds numbers in aluminum 10, 20 and 40 PPI were analyzed. The length-averaged Nusselt numbers for both oscillating and steady flows were correlated using a grouping parameter proposed by Fu et al. [17]. For the purpose of designing a novel heat sink using metal foam subjected to oscillating flow, the relation between the length-averaged Nusselt number and the pumping power of the cooling system for aluminum foam with different pore densities were analyzed.

2. Experimental methodology

2.1. Experimental facility

As shown in Fig. 2(a), an experimental facility was developed to investigate heat transfer of oscillating flow through a channel filled with aluminum foam with different pore densities. The entire setup was constructed of Teflon material and the channel was well insulated. Air was used as the working fluid. It is noted that the average maximum flow velocity and pressure drop for different oscillatory frequencies measured in the experiment were relatively low. The ranges of velocity and pressure drop were approximately 0–3.5 m/s and 0–500 Pa, respectively. Therefore, the air flow was assumed to be incompressible in the present investigation. Oscillating flow was provided by a reciprocating piston in a cylinder, which was driven by an electric motor through a crankshaft. By adjusting the motor speed through a transducer, oscillating flows of different frequencies were generated. In the experiments, oscillating frequencies from 1 to 9 Hz were employed. To focus the study on the effect of oscillatory frequency on the heat transfer in metal foam with various pore densities, the maximum flow displacement was chosen to be 68 mm which is the maximum value achievable by the present experimental setup. At the two ends of the test section, two pairs of the coolers were installed at the upper and bottom sections of the channel. One block of aluminum 10 PPI foam was inserted between two coolers to enhance the cooling effect. The heat carried by oscillating flow was transferred to the surface of coolers through the unheated aluminum foams. A hot-wire sensor was mounted at the center of the two ends packed with 40 mesh woven screen discs. The packed screen provides a uniform velocity profile so that the measured velocity is the cross-section averaged velocity through the test section. It is noted that the measured velocities will always be positive even though the velocity direction is reversed on every other half cycle as the single hot-wire sensor cannot distinguish the flow direction. To reflect a correct velocity direction, the measured values of velocity were processed by reversing its sign on every other half cycle.

Fig. 2(b) shows the three-dimensional cross-sectional view of the test section. The metal foam block of dimensions 50 (L) × 50 (W) × 10 (H) mm was tiled in the channel of width 50 mm and height 10 mm. The constant power input at the bottom of the channel was controlled by adjusting the supply voltage to the film heater, which could be monitored through the display from a digital voltmeter and an ammeter. A 1-mm-thick copper plate ($k = 384$ W/m K) with narrow slots was inserted between the metal foam and film heater for the purpose of attaching the thermocouples. Thermal grease was applied on the two sides of the copper plate as a filling material to distribute the heat evenly and to reduce the thermal contact resistance. The metal foam was clamped tightly onto the surface of copper plate by screws which secured the upper and bottom channels. This arrangement will allow the heat flux to be considered as uniform at the bottom section of the channel. The copper plate was cleaned and eight thermocouples were fixed into eight narrow slots as shown in Fig. 2(b). The locations of these thermocouples X/D_e are 0, 0.4284, 0.8568, 1.2858, 1.7142, 2.1456, 2.5716 and 3. In the experiments, it was difficult to measure the bulk air temperature inside the metal foam along the test section due to the

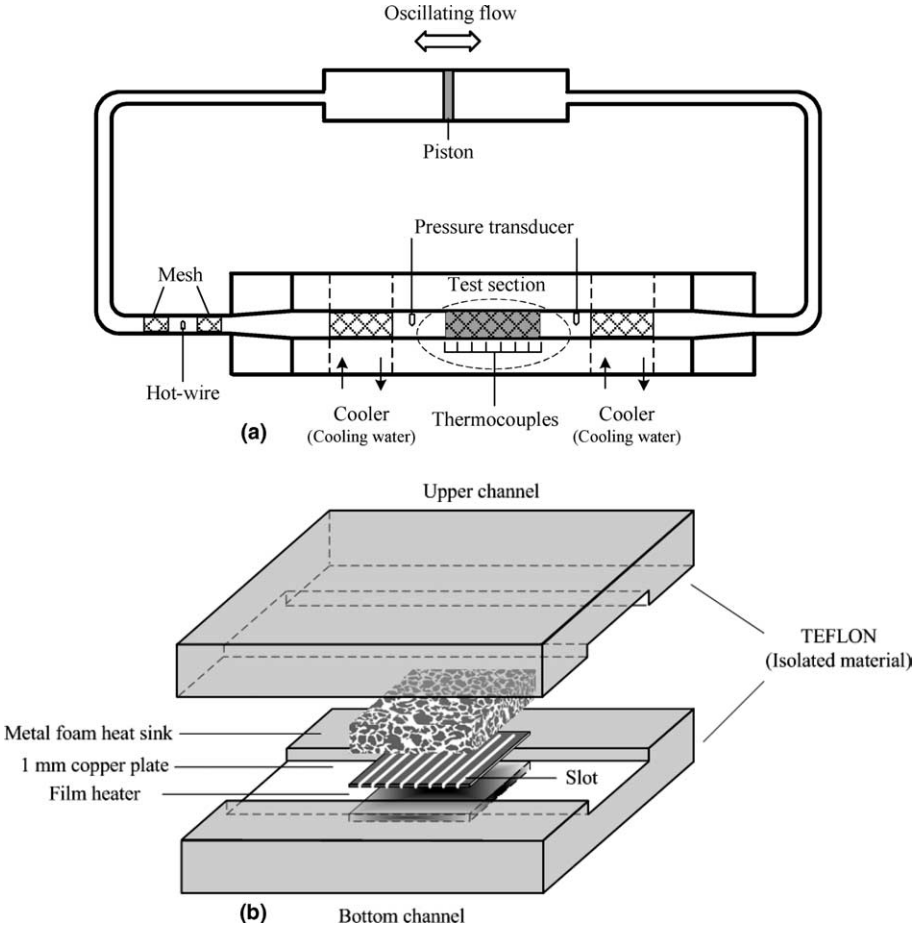

Fig. 2. (a) Sketch of experimental setup and (b) 3-D structure of test section.

compactness of the porous medium. Therefore, the inlet temperature which takes into consideration of the thermal potential for heat transfer from the heated surface to air flow was used to calculate the local Nusselt number. Two thermocouples were placed at the two ends of the test section to measure inlet bulk temperature. Type *K* thermocouples with wire diameter of 45 μm were used. The response sensitivity of these thermocouples is 40 μV/ °C which satisfied the requirements of the experiments. The two taps for the pressure sensors are located before and after the test section for pressure drop measurements. The oscillating flow facility is also capable of performing steady flow experiments. By leaving one end of the test section open to the atmosphere, experiments of steady flow through metal foam channel can be conducted through an auto-balance compressor with the same test section configuration and sensors.

Before the commencement of the experiments, all thermocouples, pressure sensors and hot-wire were carefully calibrated. By looping the test section to the oscillating piston within the cylinder, heat transfer experiments of oscillating flow can be conducted. Cooling water at room temperature was forced through the four coolers to remove the dissipated heat. The flow velocity through the test section, pressure drop across the test section and temperature distribution along the axial direction on the substrate surface were measured in the present experiments. All the signals were collected by a data acquisition system consisting of a voltage amplifier, pressure transducer, constant-temperature anemometer and a 12-bit data acquisition card within a personal computer. To obtain a cyclic steady state, the temperatures on the substrate surface were monitored by the data acquisition system. Fifty cycles of data were obtained under different sampling rates by adjusting the acquired A/D rate for different oscillating frequency. When a set of reading had been recorded, the test apparatus had to be cooled to ambient temperature of about 25 °C before the next set of experiments can be started.

2.2. Data reduction

As described previously, the current experimental facilities were designed to study oscillating flow in a metal foam channel, which possesses the reversed flow direction in every half cycle. The test section was heated uniformly at the bottom of the channel by a film heater, and two identical coolers are located at the two ends of the test sections. In the first half cycle, the fluid passes through the test section and carries the heat generated by the film heater into the unheated section where the coolers are located. The fluid temperature

drops quickly because the cooling water is forced through the coolers to remove the heat carried by oscillating flow. In the next half cycle as the fluid reverses direction, the colder fluid enters the channel to cool the test section again. Therefore, the temperatures at the various locations on the substrate surface of the channel are transient measurements. To minimize the data reduction uncertainty, the cycle-averaged method was employed to reduce the present experimental data over 50 complete cycles.

The uncertainties of the measured data can be classified into two groups: random uncertainties, which can be treated statistically; and systematic uncertainties, which cannot be treated in the same way. With careful experimentation, systematic uncertainty can be minimized. The accuracies of the thermocouple temperature and pressure transducer readings are within ±0.1 °C and ±0.25% of full-scale, respectively. The accuracy of the velocity measured by the hot-wire anemometer is ±0.01 m/s. After the cycle-averaging process, uncertainties of temperature, velocity and pressure are 3.0%, 2.0% and 2.0%, respectively. The uncertainties of D_e, d_l, f, H, and Q are estimated to be 1.0, 2.0, 2.5, 1.0 and 3.0, respectively. The uncertainties of Re_ω, Nu_x and W_p were determined by the method described by Taylor [18]. If $v,\ldots,y,\ldots,z$ are measured quantities with uncertainties $\delta v,\ldots,\delta y,\ldots,\delta z$, and the measured values are used to compute the function $q(v,\ldots,y,\ldots,z)$, then the uncertainty in q is

$$\delta q = \sqrt{\left(\frac{\partial q}{\partial v}\delta v\right)^2 + \cdots + \left(\frac{\partial q}{\partial y}\delta y\right)^2 + \cdots + \left(\frac{\partial q}{\partial z}\delta z\right)^2} \quad (1)$$

In the present experiments, the uncertainties of the measured data were assumed to be independent and random with normal distribution. Using Eq. (1), the uncertainties of Re_ω, Nu_x and W_p are calculated to be 3.9%, 5.7% and 2.8%, respectively.

3. Results and discussion

3.1. Physical properties of aluminum foams

As mentioned in a previous section, the tested aluminum foam was fabricated by the infiltration casting technique in which a solid mold of pore shapes is made before molten metal is poured into the mold. Therefore, the ligament figure can be controlled carefully and the diameters of ligaments inside the metal foam can be considered to be of equal size. In the present study, the ligament diameter of the tested aluminum foam was measured by a scanning electron microscope. The average diameter of ten ligaments measured randomly was used as the ligament diameter in the calculation. For the present metal foam, the effective porosity is equal to the porosity due to the metal foam with fully connected pore structure, i.e. no dead end and isolated pores. The porosity ε, calculated by dividing the weight of the foam by its volume (determined from the external dimensions) is given by

$$\varepsilon = \frac{v_t - v_s}{v_t} \quad (2)$$

where v_t is the total volume and v_s is the volume of solid fraction of porous material.

The inertial coefficient describes the effects of the local aspects of the pore space morphology on the flow momentum transport in the porous media. The permeability is the measure of the flow conductance of the porous matrix, which relates the averaged flow velocity through the pores with pressure drop in porous media. The critical properties of permeability K and inertia coefficient F of the tested metal foams were obtained by applying the quadratic curve fitting method to pressure drop versus fluid velocity data obtained under steady flow conditions. The following relation between measured pressure drop and flow velocity is derived:

$$\frac{\Delta P}{L} = AU + BU^2 \quad (3)$$

where ΔP is the pressure drop across the media, L is the length of the media, and U is average flow velocity in the metal foam channel. The two coefficients of A and B are defined as

$$A = \frac{\mu_f}{K}, \quad B = \rho_f \frac{F}{\sqrt{K}} \quad (4)$$

where μ_f and ρ_f are the dynamic viscosity and density of the fluid, respectively. Fig. 3 presents the data of pressure drop per unit length versus velocity for steady flow through the aluminum 10, 20 and 40 PPI foams. By fitting the second-order polynomial of Eq. (3) through the data points, coefficients A and B can be determined. By substituting the values of A and B into Eq. (4), the corresponding values for permeability K and inertia coefficient F can be determined. The critical parameters of the tested aluminum foams are listed in Table 1. The effective thermal conductivities of aluminum foams were obtained by the model presented by Boomsma and Poulikakos [19], which is a geometrical effective thermal conductivity model based on

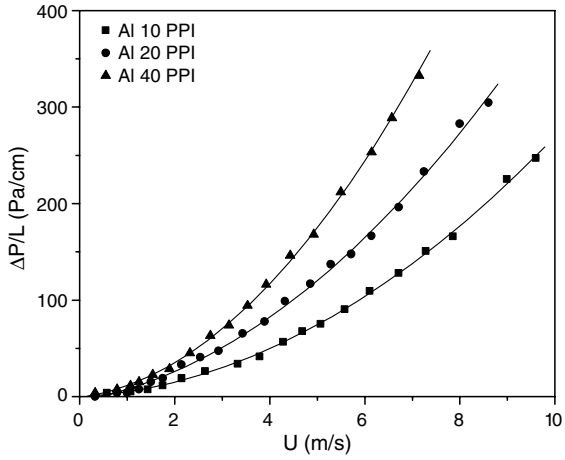

Fig. 3. Pressure drop versus velocity of steady flow in aluminum 10, 20 and 40 PPI.

Table 1
Physical properties of aluminum foams

Physical properties	Al 10 PPI	Al 20 PPI	Al 40 PPI
Ligament diameter, d_l (μm)	427.2	221.3	112.6
Porosity, ε	0.91	0.90	0.90
Effective thermal conductivity, k (W/m K)	4.1	5.1	5.9
Specific surface area, α ($m^2\,m^{-3}$)	820	1700	2800
Inertia coefficient, F	0.0076	0.0105	0.0155
Permeability, K ($10^{-8}\,m^2$)	4.21	3.12	2.86

the idealized three-dimensional cell structure of the tetrakaidecahedron.

3.2. Pressure drop

To study the effect of oscillatory frequency on pressure drop, the kinetic Reynolds number Re_ω defined based on the oscillatory frequency f is employed as

$$Re_\omega = \frac{2\pi f D_e^2}{\nu_f} \tag{5}$$

where $D_e = 5H/3$ is the hydraulic diameter of channel, ν_f is kinematic viscosity of the fluid and H is the height of the channel.

The effect of kinetic Reynolds number on pressure drop across the aluminum 40 PPI foam are shown in Fig. 4 for a complete cycle at $Re_\omega = 301$, 479 and 687. The profiles of pressure drop under different kinetic Reynolds numbers are nearly sinusoidal in shape due to the reciprocating motion of the driving piston. It can be seen that the pressure drop for high kinetic Reynolds number (high frequency) is much higher than that for low kinetic Reynolds number (low frequency). Fig. 5 shows the variations of pressure drop in aluminum foams of 10, 20 and 40 PPI. The oscillatory frequency was set to 4 Hz, i.e., the kinetic Reynolds number $Re_\omega = 425 \sim 436$ for aluminum 10, 20 and 40 PPI. It is observed that the profiles of pressure drop gradually increase with the increase of the foam's pore density.

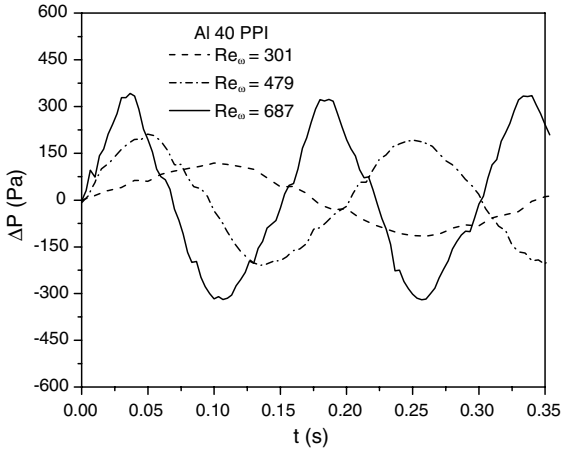

Fig. 4. Transient pressure drop of oscillating flow in aluminum 40 PPI at $Re_\omega = 301$, 479 and 687.

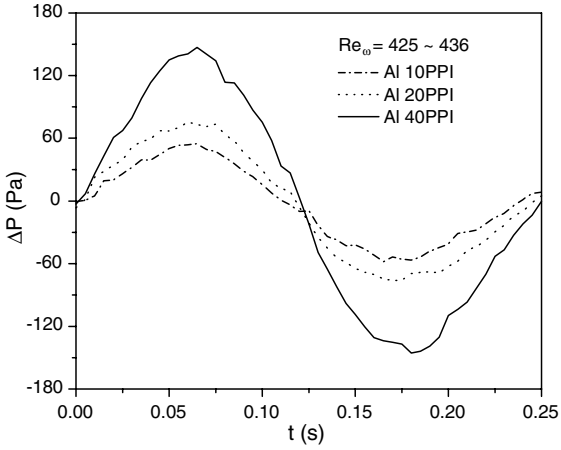

Fig. 5. Variation of pressure drop of oscillating flow in aluminum foam 10, 20 and 40 PPI at $Re_\omega = 425$–436.

The variations of pressure drop of oscillating flow in aluminum foam for different pore densities are almost in the same cycle.

Fig. 6 shows the variations of the measured maximum pressure drop and velocity with kinetic Reynolds number for oscillating flow through aluminum 10, 20 and 40 PPI foams. The data show that the maximum pressure drops and velocities increase with increasing kinetic Reynolds number i.e. dimensionless oscillatory frequency. It can be seen that the maximum pressure drop for aluminum foam with high pore density is much higher than that for aluminum foam with low pore density. However, the data for the maximum flow velocity plotted on Fig. 5 show that the increase of velocity with the kinetic Reynolds number is not as significant as that of pressure drop. This implies that the appropriate velocity for cooling electronic components can be obtained at a relative low pressure drop by using oscillating flow through an aluminum foam heat sink. For a closer view, the large difference of the maximum pressure drop between oscillating flow through aluminum 10 and 40 PPI foam can be observed at approximately the same

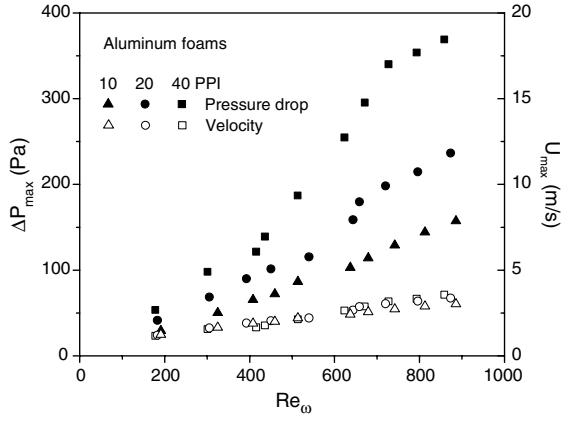

Fig. 6. Maximum pressure drop and velocity of oscillating flow through aluminum foam 10, 20 and 40 PPI with different kinetic Reynolds numbers.

flow velocity. This implies that the driving power for oscillating flow in high pore density foam has to be higher than that in low pore density foam to achieve the same flow velocity.

3.3. Heat transfer performance

To study the heat transfer performance of oscillating flow in aluminum foam with different pore densities under various kinetic Reynolds numbers, the cycle-averaged local temperature and Nusselt number are introduced in the present study. The cycle-averaged local surface temperature is defined as the average of the local wall temperatures measured for a specified number of reciprocating cycles. The cycle-averaged local Nusselt number is defined based on the cycle-averaged surface temperature as follows:

$$Nu_x = \frac{h_x D_e}{k_f} \tag{6}$$

where k_f is the thermal conductivity of the fluid. D_e and h_x are the hydraulic diameter of the channel and the local heat transfer coefficient, respectively. h_x is calculated by

$$h_x = \frac{Q}{A_{heated}(T_w - T_i)} \tag{7}$$

where T_w and T_i are the cycle-averaged local surface and the bulk air inlet temperatures, respectively. Q and A_{heated} are the power input and the heated area on the bottom of the channel, respectively.

Fig. 7 presents the cycle-averaged local surface temperature of oscillating flow through metal foam 10, 20 and 40 PPI with different kinetic Reynolds numbers at the power input of 20 W. It can be observed from the graphs, that the cycle-averaged temperature distribution decreases with an increase in Reynolds number. To express the trends clearly, the quadratic polynomial was employed to fit the experimental data. The distribution fitting curves of the local surface temperatures are convex and approximately symmetric about the center of the test section where the temperature is at the maximum due to the presence of two thermal entrances of oscillating flow in the test section. The measured maximum temperatures are located at positions $X/D_e = 1.2858$ and 1.7142 around the center of the test section. The local surface temperatures near both entrances ($X/D_e = 0$ and 3) are lower than that at the center of the test section. For instance, Fig. 7(c) shows that the local surface temperatures at $X/D_e = 1.2858$ and 1.7142 are 58.4 and 58.8 °C for a power input $Q = 20$ W and $Re_\omega = 858$, respectively. The surface temperatures of the two entrances positions $X/D_e = 0$ and 3 are 53.3 and 53.8 °C, respectively. It is also observed that the inlet and outlet bulk temperatures (isolated points plotted on Fig. 7) are much lower than the temperatures in the test section due to heat removal at the coolers located at the two ends of the test section.

Fig. 8 displays the cycle-averaged local Nusselt numbers versus the dimensionless axial distance for the cases presented in Fig. 7. The data of the local Nusselt number shown in Fig. 8 were calculated by Eq. (6) based on the cycle-averaged local surface temperature. The choice of the inlet bulk temperature to calculate the local Nusselt number takes into consideration the thermal potential for heat transfer from the heated surface to the cold fluid (air flow). It can be seen that the cycle-averaged local Nusselt number in the thermal entrance region is higher than

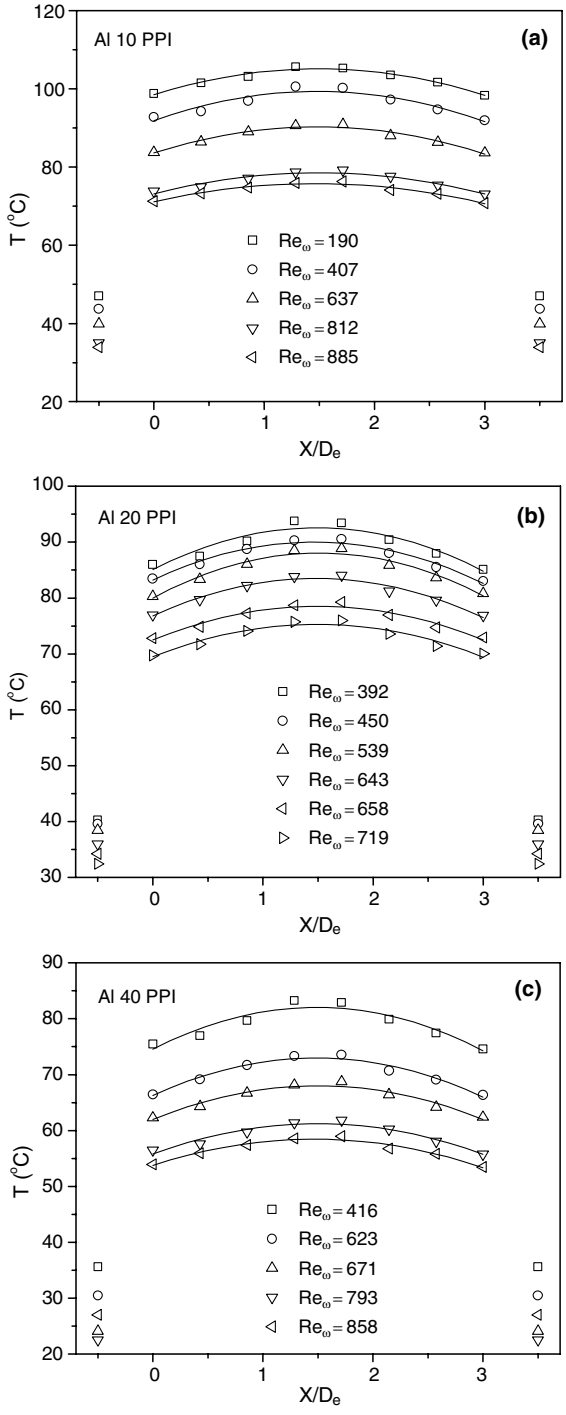

Fig. 7. Cycle-averaged temperature distributions on the substrate surface of the test section for (a) Al 10 PPI, (b) Al 20 PPI and (c) Al 40 PPI at different kinetic Reynolds numbers.

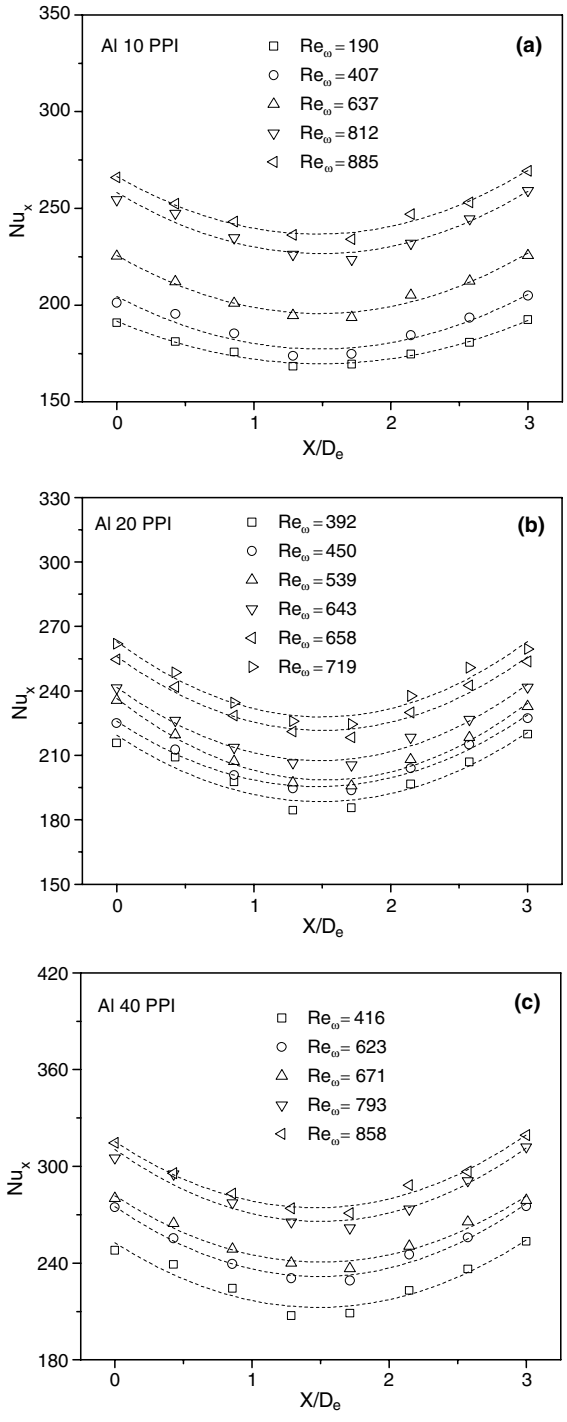

Fig. 8. Cycle-averaged local Nusselt numbers of oscillating flow through (a) Al 10 PPI, (b) Al 20 PPI and (c) Al 40 PPI with different kinetic Reynolds numbers.

that in the location around the center of the test section. As shown in Fig. 7(c) for the power input $Q = 20$ W and $Re_\omega = 858$, the cycle-averaged local Nusselt number reaches higher values of 315 and 320 at the two thermal entrances. The lower values of the averaged Nusselt number of 271 and 274 are obtained at the dimensionless lengths $X/D_e = 1.2858$ and 1.7142 around the center of the test section, respectively. As a consequence, the distribution curves of the cycle-averaged local Nusselt number for oscillating flow are concave. A similar trend was reported by Zhao and Cheng [20] in their numerical study of heat transfer in an empty tube subjected to oscillating flow.

In order to evaluate the total heat transfer rate of oscillating flow through the porous heat sink, the length-averaged Nusselt number was used to calculate the averaged Nusselt number for the whole length of the test section. Fig. 9(a) shows the averaged surface temperature along the test section for the tested aluminum foams. The averaged surface temperatures decrease with the increase of kinetic Reynolds number of oscillating flow and pore density of aluminum foam. Fig. 9(b) presents the length-averaged Nusselt number versus kinetic Reynolds number for oscillating flow through aluminum 10, 20 and 40 PPI at a power input of 20 W. It is clear that the length-averaged Nusselt number Nu_{avg} increases with the kinetic Reynolds number Re_ω i.e. the dimensionless frequency. For the same kinetic Reynolds number, the averaged Nusselt number for high pore density metal foam is higher than that for low pore density metal foam. A close-up view shows that the upward trend of the length-averaged Nusselt number is reduced with increasing kinetic Reynolds number. This

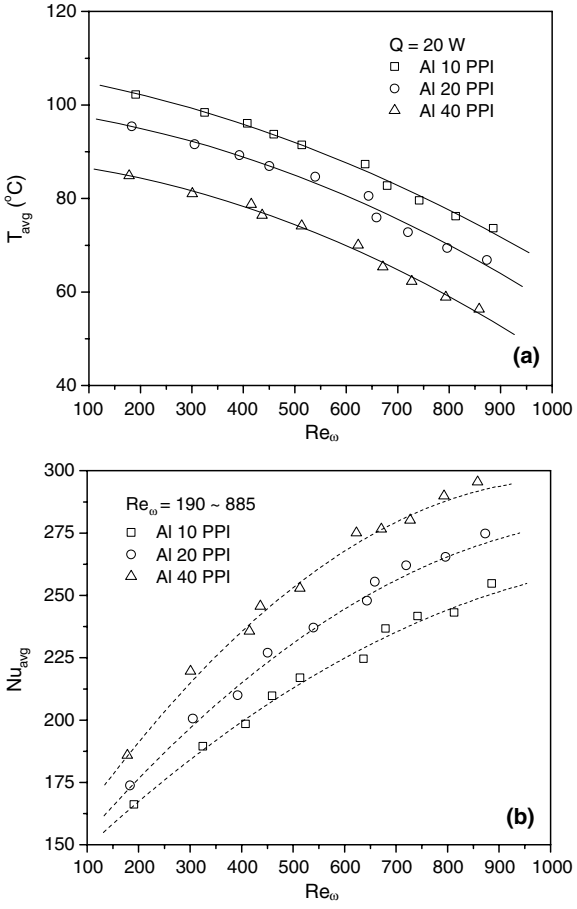

Fig. 9. (a) Length-averaged temperature and (b) length-averaged Nusselt number of oscillating flow through aluminum foam channel.

suggests that oscillating flow at relatively low frequency has a significant effect on heat transfer enhancement in a metal foam heat sink since the temperature fluctuation on the substrate surface cannot follow the oscillatory velocity at a very high frequency.

By plotting the grouping parameter $(k_e/k_f)(D_e/L)^{1/2}\,Pe_e^{1/2}$ as a function of the length-averaged Nusselt number [17], the heat transfer performance for steady and oscillating flows in metal foams can be compared. The data for the steady flow through metal foam heat sinks were obtained using the same experimental setup i.e. by connecting one end of the test section to a steady flow source (auto-balance compressor) instead of the oscillating flow generator and leaving the other end to the atmosphere. The length-averaged Nusselt number can be expressed as

$$Nu_{avg} = C\left(\frac{k_e}{k_f}\right)\left(\frac{D_e}{L}\right)^{1/2}(Pe_e)^{1/2} \tag{8}$$

where C is a constant, k_e is the effective thermal conductivity, k_f is the fluid thermal conductivity and Pe_e is the effective Peclet number. The effective thermal conductivity and effective Peclet number can be calculated as follows:

$$k_e = \phi k_f + k_d + (1-\phi)k_s, \quad k_d = \rho_f c_{pf}\gamma\sqrt{K}U \tag{9}$$

$$Pe_e = \frac{UD_e}{\alpha^*}, \quad \alpha^* = \frac{k_e}{\rho_f c_{pf}} \tag{10}$$

where k_d is the thermal dispersion conductivity, γ is the dispersion coefficient taken to be 0.025 [21] in the present study and α^* is the effective thermal diffusivity of the porous media. It should be noted that the present investigation was carried under the assumption of local thermal equilibrium due to the difficulty of determining the magnitudes of the heat fluxes obtained by the solid and fluid phases separately. Therefore, the stagnant model which includes the thermal dispersion conductivity is used to calculate the effective thermal conductivity. As shown in Fig. 10, the length-averaged Nusselt numbers for steady and oscillating flows can be collapsed into two straight lines by employing the grouping parameter. It can be seen that the length-averaged Nusselt numbers for both oscillating and steady flows increase with the grouping parameter. The slope of the line for oscillating flow is larger than that for steady flow. The constant C obtained by the present study for steady and oscillating flows are 0.34 and 0.51, respectively. The larger value of constant C for oscillating flow shows that better heat transfer performance of oscillating flow through the metal foam channel can be obtained compared to steady flow. The presence of two thermal entrance regions at the test section with higher cycle-averaged local Nusselt number results in a higher length-averaged Nusselt number for oscillating flow.

The heat transfer performances for metal foam and traditional finned heat sinks are also compared in Fig. 10. Lau and Mahajan [22] studied heat transfer of a longitudinal finned heat sink in a ducted arrangement. Their results

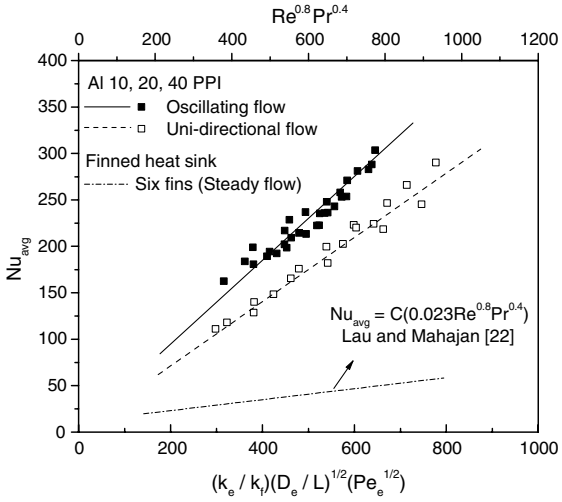

Fig. 10. Grouping parameter $(k_e/k_f)(D_e/L)^{1/2}Pe_e^{1/2}$ as a function of length-averaged Nusselt number for oscillating and steady flows through aluminum foam and comparison between metal foam and finned heat sinks.

showed that the net heat transfer rates for finned heat sinks can be expressed as

$$Nu_{avg} = C(0.023Re^{0.8}Pr^{0.4}) \tag{11}$$

where Pr is the Prandtl number and C is a constant taken to be 1.42 which took into account enhanced heat transfer due to developing flow. $Re = UD_h/\nu_f$ is the Reynolds number based on the hydraulic diameter of the fin $D_h = 4SH_f/(S+2H_f)$, where H_f and S are the height and the fin spacing of the heat sink, respectively. The average Nusselt numbers for six-fin heat sink with flow velocities ranging from 1–5 m/s subjected to steady flow are plotted as a dash-dot line in Fig. 10. It can be seen that the average Nusselt number for the finned heat sinks is much lower than that of the metal foam heat sinks, especially for aluminum foam heat sinks under oscillating flow condition. It is also observed that the increase of average Nusselt number with flow velocity for finned heat sinks is not as significant as that for aluminum foam heat sinks. These results demonstrate that significant heat transfer enhancement can be achieved by replacing traditional fin heat sinks with metal foams. The same result was also reported by Bhattacharya and Mahajan [7] in their experimental study of forced convection in metal foam heat sinks for electronics cooling.

It was noted in Fig. 6 that the differences in flow velocity for oscillating flow in aluminum 10, 20 and 40 PPI are very small for constant kinetic Reynolds number. However, a large difference in pressure drop was observed at the same time. This implies that a higher driven force is required in oscillating flow through high pore density foam in order to obtain the same flow velocity as compared to that required in low pore density foam due to the conservation of energy principle. In the design of heat sinks for cooling electronic packages, the heat removal capability of the heat sink must be assessed together with the driven force required to

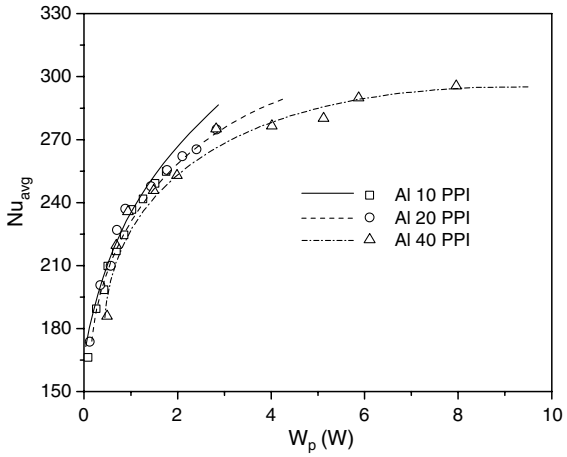

Fig. 11. Pumping power versus length-averaged Nusselt number for oscillating flow through aluminum foam 10, 20 and 40 PPI.

operate the system i.e. the pumping power. The required maximum pumping power for oscillating flow through metal foam heat sink can be calculated by

$$W_p = \Delta P_{max} \dot{V} \tag{12}$$

where W_p and $\dot{V}$ are the average maximum pumping power and volumetric flow rate, respectively. $\dot{V}$ was determined by the average maximum flow velocity through the cross-sectional area of the tested channel.

The data for the maximum pumping power versus the length-averaged Nusselt number for oscillating flow through aluminum 10, 20 and 40 PPI foams are plotted in Fig. 11. It can be seen that the relationship between the maximum pumping power and length-averaged Nusselt number is nonlinear. The pumping power increases with the length-averaged Nusselt number of oscillating flow in aluminum foam with various pore densities. The data on Fig. 11 show clearly that the high length-averaged Nusselt numbers of Fig. 9 for oscillating flow in aluminum 40 PPI are achieved at the expense of larger pumping power. The trend of fitting curves shows that the same length-averaged Nusselt number under small pumping power can be obtained by oscillating flow through aluminum foam with low pore density. It can also be observed that the increase of length-averaged Nusselt number at large pumping power is not significant, especially for high pore density aluminum foam. For example, with an increase in the average Nusselt number from 270 to 290 in aluminum 40 PPI, the pumping power is increased sharply from 3.2 to 6.2 W. At the same time, there is only 1.3 times increase in pumping power when the average Nusselt number is increased from 250 to 270. Therefore, an increase in flow rate and hence pumping power is insignificant in enhancing heat transfer of oscillating flow in a metal foam heat sink. This indicates that relatively high heat transfer performance can be obtained in low pore density metal foam subject to oscillating flow by an appropriate pumping power.

4. Conclusions

The effect of the kinetic Reynolds number on heat transfer performance of aluminum foams heat sinks of different pore densities subjected to oscillating flow was investigated. The cycle-averaged temperatures were found to decrease with an increase in the kinetic Reynolds number while the Nusselt numbers exhibit the opposite trend. A comparison of average Nusselt numbers of aluminum foam and finned heat sinks shows that better heat transfer performance can be achieved by using metal foams as heat sinks. The higher value of the constant C in the correlating equation relating the grouping parameter $(k_e/k_f)(D_e/L)^{1/2}Pe_e^{1/2}$ with the length-averaged Nusselt number for oscillating flow indicates that better heat transfer can be obtained as compared to steady flow.

For aluminum foam heat sinks, the heat transfer rate increases with the increase of the pore density at a constant kinetic Reynolds number i.e. dimensionless oscillatory frequency. However, for a given pumping power, better heat transfer performance can be achieved by low pore density metal foam under the condition of oscillating flow. In designing a novel heat sink, metal foams of low pore density can be used to enhance heat transfer with small pumping power. High pore density metal foams with their extremely large fluid–solid-contact surface areas and tortuous coolant flow paths are suitable to remove extraordinarily high heat fluxes in applications where pumping power is not of concern.

References

[1] K. Vafai, C.L. Tien, Boundary and inertia effects on flow and heat transfer in porous media, Int. J. Heat Mass Transfer 24 (1981) 195–203.
[2] M. Kaviany, Laminar flow through a porous channel bounded by isothermal parallel plates, Int. J. Heat Mass Transfer 28 (1985) 815–858.
[3] P. Cheng, C.T. Hsu, A. Choudhury, Forced convection in the entrance region of a packed channel with asymmetric heating, ASME J. Heat Transfer 110 (1988) 946–954.
[4] T.S. Zhao, P. Cheng, Oscillatory pressure drop through a woven-screen packed column subjected to a cyclic flow, Cryogenics 36 (1996) 333–341.
[5] P.X. Jiang, Z.P. Ren, B.X. Wang, Z. Wang, Forced convective heat transfer in a plate channel filled with solid particles, J. Thermal Sci. 5 (1996) 43–53.
[6] T.J. Lu, H.A. Stone, M.F. Ashby, Heat transfer in open-cell metal foams, Acta Mater. 46 (1998) 3619–3635.
[7] A. Bhattacharya, R.L. Mahajan, Finned metal foam heat sinks for electronics cooling in forced convection, ASME J. Elect. Packag. 124 (2002) 155–163.
[8] S.Y. Kim, B.H. Kang, J.H. Kim, Forced convection from aluminum foam materials in an asymmetrically heated channel, Int. J. Heat Mass Transfer 44 (2001) 1451–1454.
[9] K.H. Ko, N.K. Anand, Use of porous baffles to enhance heat transfer in a rectangular channel, Int. J. Heat Mass Transfer 46 (2003) 4191–4199.
[10] K. Boomsma, D. Poulikakos, F. Zwick, Metal foams as compact high performance heat exchangers, Mech. Mater. 35 (2003) 1161–1176.

[11] G. Hwang, C. Chao, Heat transfer measurement and analysis for sintered porous channels, ASME J. Heat Transfer 116 (1994) 456–464.
[12] K.C. Leong, L.W. Jin, Heat transfer of oscillating flow and steady flows in a channel filled with porous media, Int. Commun. Heat Mass Transfer 31 (2004) 63–72.
[13] M. Sozen, K. Vafai, Analysis of oscillating compressible flow through a packed bed, Int. J. Heat Fluid Flow 12 (1991) 130–136.
[14] Z.X. Guo, S.Y. Kim, H.J. Sung, Pulsating flow and heat transfer in a pipe partially filled with a porous medium, Int. J. Heat Mass Transfer 40 (1997) 4209–4218.
[15] K.C. Leong, L.W. Jin, An experimental study of heat transfer in oscillating flow through a channel filled with an aluminum foam, Int. J. Heat Mass Transfer 48 (2005) 243–253.
[16] K.C. Leong, L.W. Jin, Characteristics of oscillating flow through a channel filled with open-cell metal foam, Int. J. Heat Fluid Flow, in press.
[17] H.L. Fu, K.C. Leong, X.Y. Huang, C.Y. Liu, An experimental study of heat transfer of a porous channel subjected to oscillating flow, ASME J. Heat Transfer 123 (2001) 162–170.
[18] J.R. Taylor, An Introduction to Error Analysis, second ed., University Science Books, California, 1997.
[19] K. Boomsma, D. Poulikakos, On the effective thermal conductivity of a three-dimensionally structured fluid-saturated metal foam, Int. J. Heat Mass Transfer 44 (2001) 827–836.
[20] T.S. Zhao, P. Cheng, Oscillatory heat transfer in a pipe subjected to a laminar reciprocating flow, ASME J. Heat Transfer 118 (1996) 592–598.
[21] M.L. Hunt, C.L. Tien, Effects of thermal dispersion on forced convection in fibrous media, Int. J. Heat Mass Transfer 31 (1988) 301–309.
[22] K.S. Lau, R.L. Mahajan, Effects of tip clearance and fin density on the performance of heat sinks for VLSI packages, IEEE Trans. Compon. Hybrids. Manuf. Technol. 12 (1989) 757–765.